

1 **Exceptionally well-preserved Cretaceous microfossils reveal new biomineralization styles**

2

3 Jens E. Wendler<sup>1,2</sup> and Paul Bown<sup>3</sup>

4

5 <sup>1</sup>Department of Paleobiology, MRC-121, Smithsonian Institution, 10<sup>th</sup> and Constitution Ave,  
6 Washington D.C. 20560, USA

7 <sup>2</sup>Department of Geosciences, Bremen University, P.O. Box 330440, 28334 Bremen, Germany

8 <sup>3</sup>Department of Earth Sciences, University College London, Gower Street, London WC1E 6BT,  
9 UK

10 Correspondence and requests for materials should be addressed to J.E.W. [wendler@uni-](mailto:wendler@uni-bremen.de)  
11 [bremen.de](mailto:wendler@uni-bremen.de).

12

13 **Calcareous microplankton shells form the dominant components of ancient and modern**  
14 **pelagic sea-floor carbonates and are widely used in palaeoenvironmental reconstructions.**  
15 **The efficacy of these applications, however, is dependent upon minimal geochemical**  
16 **alteration during diagenesis, but these modifying processes are poorly understood. Here we**  
17 **report on new biomineralization architectures of previously unsuspected complexity in**  
18 **calcareous cell-wall coverings of extinct dinoflagellates (pithonellids) from a Tanzanian**  
19 **microfossil-lagerstätte. These Cretaceous ‘calcispheres’ have previously been considered**  
20 **biomineralogically unremarkable but our new observations show that the true nature of**  
21 **these tests has been masked by recrystallization. The pristine Tanzanian fossils are formed**  
22 **from fibre-like crystallites and show archeopyles and exquisitely constructed opercula,**  
23 **demonstrating the dinoflagellate-affinity of pithonellids, which has long been uncertain.**

24 **The interwoven fibre-like structures provide strength and flexibility enhancing the**  
25 **protective function of these tests. The low-density wall fabrics may represent specific**  
26 **adaptation for oceanic encystment life-cycles, preventing the cells from rapid sinking.**

27

28 Calcification is rare in eukaryotes but has arisen separately as a cell-wall covering in the  
29 coccolithophore, foraminifera, and dinoflagellate marine protistan plankton groups<sup>1</sup>. These  
30 calcareous shells are widely used as environmental proxies and age-dating tools but despite these  
31 widespread geoscientific applications, their biomineralization is relatively poorly understood  
32 because it is difficult to maintain most living taxa in culture and their fossils are generally  
33 modified by diagenetic recrystallization of fine-scale primary structures. Calcareous shells of  
34 dinoflagellates are mostly spherical calcite tests (~10-180  $\mu\text{m}$ ) formed by the family  
35 Thoracosphaeraceae<sup>2</sup> living in shelf and oceanic surface waters. Around 30 living species and  
36 260 fossil species are known, with most extant forms producing calcareous immotile coccoid  
37 cells some of which function as reproductive resting cysts<sup>2,3</sup>. The simple fossil forms that have  
38 been included in the calcareous dinoflagellates have wall-architectures with randomly-oblique,  
39 radial, tangential, and inclined-radial (pithonellid) crystallographic orientations<sup>4</sup>. Specimens of  
40 uncertain biological affinity, lacking diagnostic dinoflagellate characters, have been termed  
41 calcispheres or calcitarchs<sup>5</sup> and include the extinct Cretaceous pithonellids. Here we show  
42 unsuspected ultrastructural complexity and morphological traits in pithonellid fossils, which  
43 have been previously unidentified due to the masking effects of diagenesis. These new structures  
44 shed light on the biological affinity of pithonellids and the biomineralogical functionality of their  
45 calcareous cell-wall coverings.

46

47 **Results**

48 **Pithonellids – the dominant Cretaceous calcispheres.** The extinct pithonellid forms dominate  
49 late Cretaceous calcisphere assemblages and can occur in rock-forming abundance<sup>6-8</sup>. Prior to  
50 this study, their biomineralogically unremarkable architecture (Fig. 1a) and lack of unequivocal  
51 morphological features that characterise dinoflagellates (e.g., tabulation and archeopyles) raised  
52 doubts concerning their true biological affiliation<sup>2,3,5</sup>. Most of these forms have appeared to be  
53 constructed from two single-layered walls of coarse (>1µm), equidimensional calcite crystallites,  
54 although specimens showing variable crystallite size and multiple wall-layers have been  
55 observed infrequently and considered to represent ecophenotypic or intraspecific variability<sup>9,10</sup>.  
56 Our new observations come from material initially targeted for its preservation of unaltered  
57 foraminiferal calcite and used to generate high quality geochemical palaeoclimate proxy records  
58 for the Palaeogene<sup>11,12</sup>. Geochemical evidence, but also the extraordinary preservation of  
59 coccolithophore calcareous microfossils<sup>13</sup>, have demonstrated the exceptional nature of the  
60 carbonate preservation in the Tanzanian sediments. Our new results come from Turonian (89–93  
61 Ma)<sup>14</sup> sediments that are 30 million years older and extend this microfossil lagerstätte record  
62 into the Cretaceous.

63 **Pithonellid ultrastructure.** The Tanzanian pithonellid fossils are incomparably better preserved  
64 than any previously documented specimens<sup>15</sup> yet they are assignable to known species based on  
65 their gross morphology and crystallographic orientation (Fig. 1b, c). Thus, we can show that the  
66 pristine pithonellid walls (Fig. 1d) are constructed from minute (~0.1µm wide), rod-like  
67 crystallites, often in groups of similar orientation (Fig. 1e-g), which are arranged in patchwork-  
68 like, partly interwoven patterns (Fig. 1f, h). These layers form a submicron-scale lamination of

69 the shell-wall (Fig. 1d, h). Sub-angular, circular and slit-like perforations are typical and often  
70 outlined by concentrically-arranged crystallites (Figs. 1g; 2).

71

## 72 **Discussion**

73 These new observations suggest that most, if not all, previously described pithonellid-type  
74 microfossils have been strongly modified by recrystallization and bear little resemblance to their  
75 primary architectures. Importantly, we have observed large, taxonomically-diagnostic circular to  
76 sub-angular openings (Fig. 1g) and corresponding plate-like coverings (Fig. 1f, i, j). These  
77 openings, called archeopyles, and their associated covering plates, called opercula, are  
78 characteristic of the immotile cells of dinoflagellates and are related to hatching (excystment) of  
79 new motile cells. The presence of distinct apical archeopyles is compelling evidence for the  
80 dinoflagellate affinity of the extinct Cretaceous microfossils shown here.

81 The dinoflagellate affinity of these fossils is also supported by the observation of interwoven  
82 sub-micron scale crystallite wall-fabrics and the resulting laminated wall-architecture, which is  
83 comparable to that seen in certain living dinoflagellates, particularly, *Leonella granifera* (Fig.  
84 2d-f). The characteristic interlocking of individual crystals that form the rod-like patterns is seen  
85 in both *L. granifera* cysts (Fig. 2e) and pithonellids (Fig. 3a). Study of extant calcareous  
86 dinoflagellates has shown that biomineralization is initiated as crystal-like particles of calcite  
87 within cytoplasmic vacuoles, which then move to the cell periphery and deposit the crystals in a  
88 layer or matrix surrounding the cell <sup>16</sup>. The shell of the coccoid cells of *Leonella* has one matrix  
89 <sup>16</sup> and shows no layering while the multi-layered construction of pithonellids suggests a complex  
90 matrix consisting of multiple organic layers.

91 The fine-crystalline interwoven and fibre-reinforced, perforate, laminated fabric of pithonellids  
92 (Fig. 3b) forms a shell-construction that provides a balance of strength and flexibility, which is  
93 crucial for maximum resilience and thus protection of the cell. Similar woven fibre structures are  
94 also seen elsewhere in biominerals, such as, sea urchin tooth calcite<sup>17</sup>. In particular, near  
95 identical structure is seen in vertebrate dental enamel fabric (Fig. 3c), where it is largely  
96 responsible for the resilience of these structures, made of an otherwise inherently weak material  
97 <sup>18</sup> yielding potential applications in biomimetics<sup>17</sup>. Furthermore, such low-density  
98 biocalcification is likely a specific adaptation for oceanic encystment life cycles, preventing the  
99 cysts from sinking below the photic zone to water depths from which they could not recover  
100 following excystment.

101

## 102 **Methods**

103 **Material and field procedures.** The studied specimens were recovered from a borehole drilled  
104 during the 2007 phase of the Tanzanian Drilling Project (TDP). Drill Site TDP 22 is situated at  
105 10°04'39.4'' S / 39°37'33.5'' E and recovered lower through middle Turonian sediments (upper  
106 *Whiteinella archaeocretacea* and *Helvetoglobotruncana helvetica* planktic foraminiferal  
107 biozones)<sup>19</sup>. The sediments are unconsolidated siltstones with a carbonate content typically  
108 ranging from 10-15 wt. %. Samples were disaggregated in tap water at the drill site and size-  
109 fraction-separated over 20, 63, 125 and 250 µm sieves.

110 **Analyses.** Calcispheres were picked from the 20-63 µm size-fraction (5-10 mg per sample) with  
111 an eyelash attached to a pen. Microscope magnification was ca. 100x. Scanning electron  
112 microscopy (SEM) was performed on a Phillips XL-30 ESEM with a LaB6 electron source. The  
113 microscopic analysis comprised four steps. First the whole specimen was documented with

114 reflected light-optical imaging using a Nikon SMZ1500 binocular light microscope and multiple-  
115 plane integrated imaging with NIS Elements™ imaging software. Second, transmitted polarized  
116 light optical investigation facilitated identification of the crystallographic wall-type using a Leitz  
117 Ortholox binocular microscope after transferring specimens onto a glass slide. An eccentric  
118 extinction cross (Fig. 1C) indicates an inclined-radial (pithonellid) crystallographic orientation.  
119 Third, specimens were mounted on stubs for SEM imaging of the whole cysts and surface  
120 morphology and traits. Fourth, the specimens were opened, using a scalpel, to examine internal  
121 wall structure and inner surfaces of the cyst.

122

### 123 **References**

- 124 1 Knoll, A. H. in *Biomineralization* Vol. 54 *Reviews in Mineralogy and Geochemistry* (eds  
125 P.M. Dove, J.J. De Yoreo, & S. Weiner) Ch. 11, 381 (Mineralogical Society of America,  
126 2003).
- 127 2 Elbrächter, M. *et al.* Establishing an Agenda for Calcareous Dinoflagellate Research  
128 (Thoracosphaeraceae, Dinophyceae) including a nomenclatural synopsis of generic  
129 names. *Taxon* **57**, 1289-1303 (2008).
- 130 3 Streng, M., Hildebrand-Habel, T. & Willems, H. A proposed classification of archeopyle  
131 types in calcareous dinoflagellate cysts. *J. Paleontol.* **78**, 456-483 (2004).
- 132 4 Keupp, H. Die kalkigen Dinoflagellatenzysten des Mittelalb bis Untercenoman von  
133 Escalles/Boulonnais (N-Frankreich). *Fazies* **16**, 6-21 (1987).
- 134 5 Versteegh, G. J. M., Servais, T., Streng, M., Munnecke, A. & Vachard, D. A discussion  
135 and proposal concerning the use of the term calcispheres. *Palaeontology* **52**, 343-348  
136 (2009).

- 137 6 Wendler, J. E., Gräfe, K. U. & Willems, H. Reconstruction of mid-Cenomanian orbitally  
138 forced palaeoenvironmental changes based on calcareous dinoflagellate cysts.  
139 *Palaeogeogr. Palaeocl.* **179**, 19-41 (2002).
- 140 7 Dias-Brito, D. Global stratigraphy, palaeobiogeography and palaeoecology of Albian–  
141 Maastrichtian pithonellid calcispheres: impact on Tethys configuration. *Cretaceous Res.*  
142 **21**, 315-349 (2000).
- 143 8 Wendler, J. E., Gräfe, K. U. & Willems, H. Palaeoecology of calcareous dinoflagellate  
144 cysts in the mid-Cenomanian Boreal Realm: implications for the reconstruction of  
145 palaeoceanography of the NW European shelf sea. *Cretaceous Res.* **23**, 213-229 (2002).
- 146 9 Kohring, R., Gottschling, M. & Keupp, H. Examples for character traits and  
147 palaeoecological significance of calcareous dinoflagellates. *Paläont. Z.* **79**, 79-91 (2005).
- 148 10 Keupp, H. & Kienel, U. Wandstrukturen bei Pithonelloideae (Kalkige Dinoflagellaten-  
149 Zysten): Biomineralisation und systematische Konsequenzen. *Abh. Geol. B.-A.* **50**, 197-  
150 217 (1994).
- 151 11 Pearson, P. N. *et al.* Warm tropical sea surface temperatures in the Late Cretaceous and  
152 Eocene epochs. *Nature* **413**, 481-487 (2001).
- 153 12 Pearson, P. N., Foster, G. L. & Wade, B. S. Atmospheric carbon dioxide through the  
154 Eocene / Oligocene climate transition. *Nature* **461**, 1110-1113 (2009).
- 155 13 Bown, P. R. *et al.* A Paleogene calcareous microfossil Konservat-Lagerstätte from the  
156 Kilwa Group of coastal Tanzania. *Geol. Soc. Am. Bull.* **120**, 3-12 (2008).
- 157 14 Wendler, I., Huber, B. T., MacLeod, K. G. & Wendler, J. E. Stable oxygen and carbon  
158 isotope systematics of exquisitely preserved Turonian foraminifera from Tanzania -  
159 understanding isotope signatures in fossils. *Mar. Micropaleontol.* (in press).

- 160 15 Wendler, J. E., Wendler, I., Huber, B. T. & Rose, T. Using cathodoluminescence  
161 spectroscopy of Cretaceous calcareous microfossils to distinguish biogenic from early-  
162 diagenetic calcite. *Microsc. Microanal.* **18**, 1-9 (2012).
- 163 16 Zinssmeister, C., Keupp, H., Tischendorf, G., Kaulbars, F. & Gottschling, M.  
164 Ultrastructure of Calcareous Dinophytes (Thoracosphaeraceae, Peridiniales) with a Focus  
165 on Vacuolar Crystal-Like Particles. *PloS one* **8**, e54038 (2013).
- 166 17 Gower, L. B. Biomimetic Model Systems for Investigating the Amorphous Precursor  
167 Pathway and its Role in Biomineralization. *Chem. Rev.* **108**, 4551-4627 (2008).
- 168 18 Chai, H., Lee, J. J.-W., Constantin, P. J., Lucas, P. W. B. R. & Lawn, B. R. Remarkable  
169 resilience of teeth. *P. Natl. Acad. Sci. USA* **106**, 7289-7293 (2009).
- 170 19 Jiménez Berrocoso, Á. *et al.* Lithostratigraphy, biostratigraphy and chemostratigraphy of  
171 Upper Cretaceous sediments from southern Tanzania: Tanzania Drilling Project Sites 21  
172 to 26. *J. Afr. Earth Sci.* **57**, 47-69 (2010).

173

#### 174 **Acknowledgements**

175 This research was supported by DFG fund WE 4587/1-1 (Wendler) and the Natural Environment  
176 Research Council (Bown). Ines Wendler, Sebastian Meier, Gerard Versteegh, Jeremy Young,  
177 Helmut Willems and Brian Huber are kindly thanked for conversations and comments on the  
178 manuscript. We thank Monika Kirsch for discussion on extant calcareous dinoflagellates and  
179 providing culture material. We acknowledge the Tanzania Petroleum Development Corporation,  
180 and particularly Dr. Joyce Singano, for logistical support and the Tanzania Commission for  
181 Science and Technology for permission to drill.

182



183 **Author Contributions**

184 J.E.W. carried out the palaeontological analyses, imaging, wrote the paper and created figures.

185 P.B. was involved in fieldwork, project organization, palaeontological analyses, wrote the paper  
186 and discussed the results with J.E.W.

187

188 **Additional information**

189 **Reprints and permission:** Reprints and permissions information are available at

190 [www.nature.com/reprintsand\\_permissions](http://www.nature.com/reprintsand_permissions).

191 **Competing financial interests:** The authors have no competing financial interests.

192

193 **Figure legends**

194 **Figure 1 | New biomineralization styles in fossil pithonellids from Tanzanian Drill Site TDP**

195 **22. (a)** *Pithonella* sp.; recrystallized cyst showing spiral rows of prismatic crystals masking  
196 primary surface traits. **(b, c)** *Pithonella lamellata* (60 specimens investigated); pristine cyst with  
197 smooth surface, an archeopyle, spiralling fine striations, and perforations. **(c)** Optical imagery,  
198 reflected light (upper) and polarized light (lower). **(d)** Wall-section showing ply-like multiple  
199 layers of sub-micron scale, fibre-like crystallites. **(e)** Inner cyst-surface fabric and pore with  
200 sieve-like cover. **(f)** Inner cyst-surface with operculum constructed of sub-micron, concentrically  
201 interwoven crystallites. **(g)** *Bonetocardiella* sp.; inner cyst-surface with archeopyle, interwoven  
202 arrangement of the lamellar wall-crystallite patchwork and circular perforations. **(h)** Archeopyle  
203 wall showing rope-like interwoven crystallite bundles and winding architecture. **(i, j)** *Pirumella*  
204 *multistrata* (120 specimens investigated), a calcareous dinoflagellate cyst of the randomly-

205 oblique wall-architecture from TDP Site 22 for comparison; operculum constructed of randomly-  
206 oblique, fibre-like crystallites. Scale bars 5  $\mu\text{m}$ .

207

208 **Figure 2 | Perforation types and comparison with extant calcareous dinoflagellates. (a, b, c)**

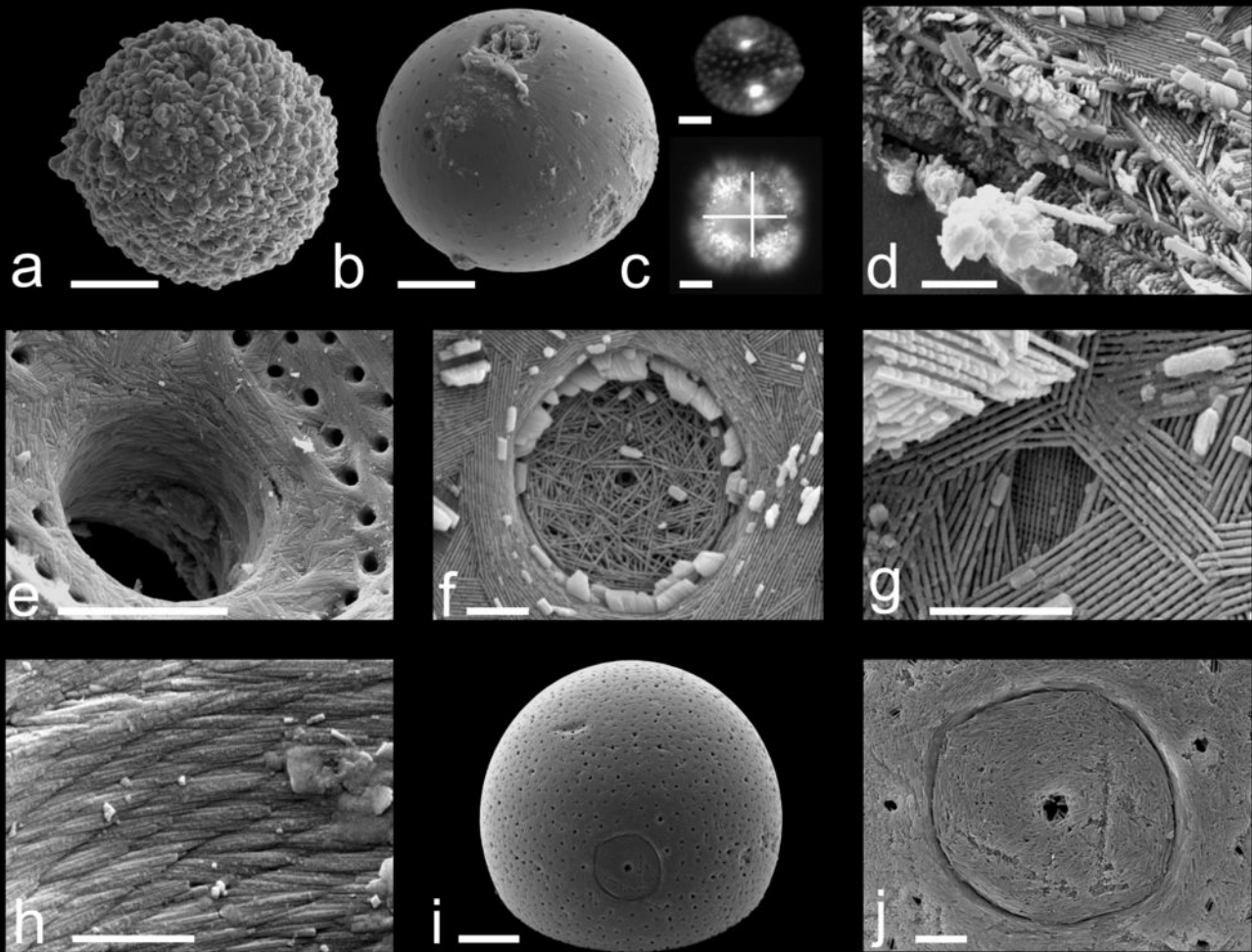
209 *Bonetocardiella* sp. from TDP Site 22 with sub-angular perforations. (b) Wall micro-fabrics in  
210 tangential, slightly oblique section. (c) Operculum. (d, e, f) *Leonella granifera* (extant species  
211 from culture, 8 specimens studied) showing circular perforations. (e) Tangential section of wall  
212 micro-fabrics consisting of an array of interlocking individual crystals forming a laminated wall,  
213 scale bar 2 $\mu\text{m}$ . (f) Operculum. (g, h, i) *Pithonella ovalis* (238 specimens studied), the type  
214 species of the genus *Pithonella*, from TDP Site 22. (h) Wall micro-fabrics of parallel fibre-like  
215 crystallites and slit-like perforations. (i) operculum. Scale bars a-d and f-i 5  $\mu\text{m}$ .

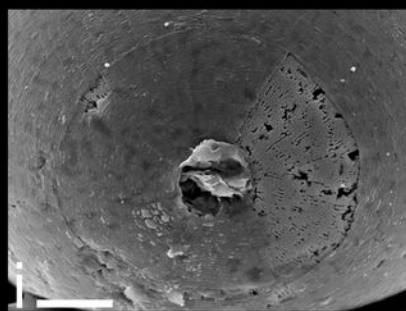
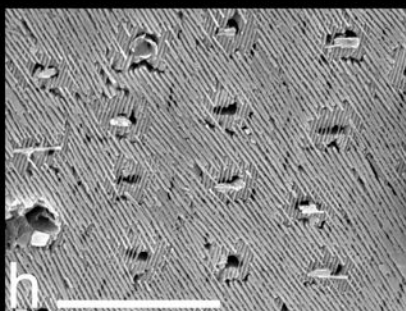
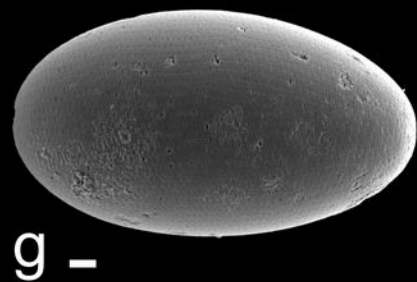
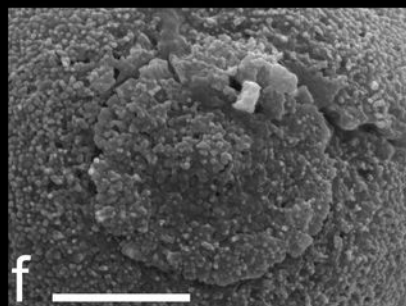
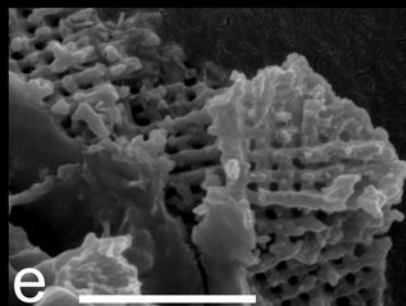
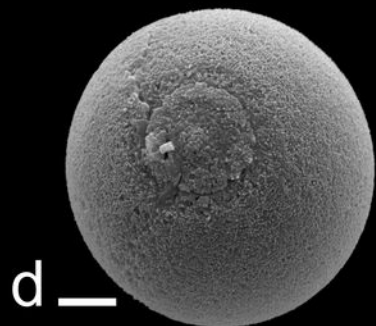
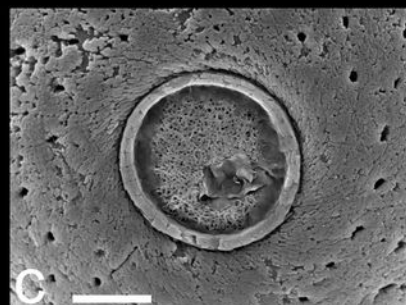
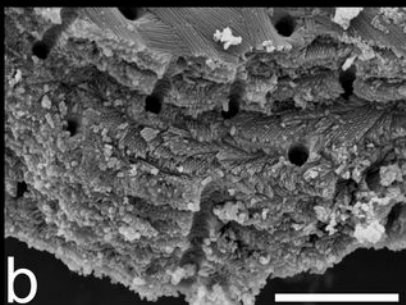
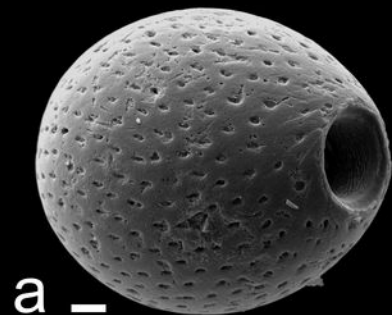
216

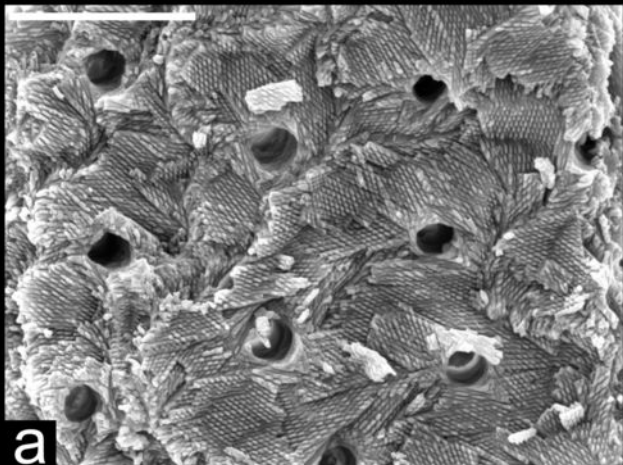
217 **Figure 3 | Ultrastructure of the pithonellid biomineral architecture and comparison to**

218 **vertebrate enamel. (a)** Tangential, slightly oblique section of *Bonetocardiella* sp. (TDP Site 22)  
219 shows various planes of the wavy lamination (seen in cross-section in figure 1h) of the cyst-wall.  
220 Note the interlocking of the individual calcite crystals resembling textile fabrics, scale bar 5  $\mu\text{m}$ .  
221 (b) Inner shell surface view of the pithonellid fibre-like, and laminated fabric around an enlarged  
222 sieve-like perforation formed by orthogonal interlocked crystallites, scale bar 1  $\mu\text{m}$ . (c) Cross-  
223 ply structure of densely interwoven fibres of rat enamel, scale bar 10  $\mu\text{m}$  (image reproduced  
224 courtesy of Dr. Laurie B. Gower, <http://gower.mse.ufl.edu/research.html>)

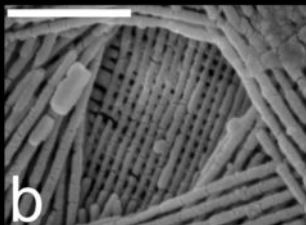
225



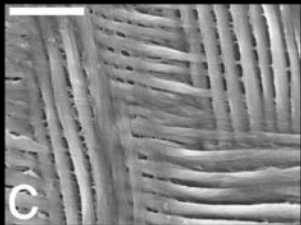




a



b



c